CHEMICAL ENGINEERING TRANSACTIONS
VOL. 81, 2020

A publication of AIDIC
The Italian Association of Chemical Engineering
Online at www.cetjournal.it

Guest Editors: Petar S. Varbanov, Qiuwang Wang, Min Zeng, Panos Seferlis, Ting Ma, Jiří J. Klemeš

ISBN 978-88-95608-79-2; **ISSN** 2283-9216

DOI: 10.3303/CET2081032

Sliding Mode Control Design of Battery Energy Storage Charging System Based on Isolated DC-DC Converter

Mingyuan Ma, Ningfan Zhong*, Meng Zhang

College of Electrical Engineering and Automation, Shandong University of Science and Technology, Qingdao 266510, China
nf_zhong@sdust.edu.cn

Battery has been widely used in the storage of new energy. In this paper, we focus on the research of the controller design of a battery charging system, in which an isolated dual converter is used for energy conversion. In practical applications, the performance of the battery charging system is always affected by the uncertain circuit parameters. In order to improve its dynamic and steady performance under various uncertainties, a sliding mode control (SMC) strategy is proposed in this paper for the control of the battery charging system. First, the working principle of the isolated dual converter with parameter uncertainties is analyzed in this paper. Then, based on the model of the battery charging system, a SMC strategy based on the Pulse Width Modulation (PWM) method is designed and analyzed in this paper. The influence of variation of switching frequency on the controller parameters design is also discussed in this paper. Finally, simulation results show that, compared with the existing method, the control strategy proposed in this paper is robust to the system parameter uncertainties and the close loop battery charging system has better transient and steady performance.

1. Introduction

In recent years, with the development and popularization of micro-grid, research on small-capacity distributed power sources has received widespread attention, especially photovoltaic. However, photovoltaic power generation is affected by changes in natural conditions such as sunlight intensity and ambient temperature and cannot continuously and stably output electric energy. Whether it is an independent or grid-connected photovoltaic system, energy storage is needed to improve the instability of its power generation (Matwankar and Alam, 2019). Independent photovoltaic power generation systems mainly use battery energy storage technology, and batteries have great potential in photovoltaic power generation applications. How to charge it reliably and efficiently has been a hot topic of research (Zheng, 2018).

Normal batteries need to store a voltage of 12V - 24V, so a buck converter with a high step-down ratio is needed to realize it (Na and Lee, 2011). In this case, an isolated DC-DC buck converter with a high-frequency transformer with a high step-down ratio may be a good choice because a non-isolated DC-DC buck converter may have difficulty simply changing the duty to achieve such a high step-down ratio. Its topology has the following two advantages (Yao et al., 2015): (1) adding a transformer between the input and output to achieve electrical isolation, reducing mutual interference between the high-voltage and low-voltage sides; (2) leakage inductance of the transformer or the series inductance of the primary side and the parasitic capacitance of the switch tube can be used to realize the zero voltage switch (ZVS) of the switch tube. Compared with traditional hard switching, this soft switching technology can reduce the loss of the switch tube, improving the efficiency of the switching power supply. In recent years, the application range of isolated full-bridge DC-DC converters has been expanding, including applications in photovoltaic systems, DC power systems, energy storage systems for electric vehicles, and charging and discharging between batteries and super capacitors.

The main goal of its control strategy is to ensure the stability of the system in any situation, and to have a good dynamic response in suppressing input voltage changes, load changes, and parameter uncertainty. Because of simplicity and less cost, several industries use linear controllers like PI or PID control for regulating isolated DC-DC converters. For parameters variations like huge variations in load or input voltage these controllers are not robust. So linear control methods are not suitable for isolated DC-DC converters. Since the isolated DC-DC

Paper Received: 31/03/2020; Revised: 31/05/2020; Accepted: 04/06/2020
Please cite this article as: Ma M., Zhong N., Zhang M., 2020, Sliding Mode Control Design of Battery Energy Storage Charging System Based on Isolated DC-DC Converter, Chemical Engineering Transactions, 81, 187-192 DOI:10.3303/CET2081032

converter is a nonlinear time-varying system, nonlinear controllers are appropriate for controlling DC-DC converters. Stable transient response can be obtained under the various conditions by using these nonlinear controllers. Various nonlinear control strategies have been used to control isolated DC-DC converters, such as adaptive control, artificial neural network control, fuzzy control, hierarchical control. etc. (Ding et al., 2018). Among these nonlinear control strategies, sliding mode control (SMC) (Yu and Kaynak, 2017) has received extensive attention for its advantages such as ensuring stability, robustness to parameter changes, fast dynamic response, and simple implementation (Naik and Mehta, 2017). In this paper, the PWM based sliding mode controller is used to adjust the isolated DC-DC converter, so that the battery can charge stably and continuously under any conditions.

2. State space model of transformer

The isolated full-bridge DC-DC converter is shown in Figure 1.

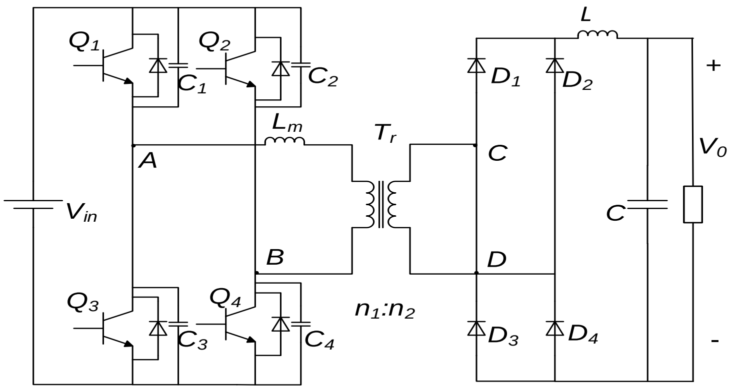

Figure 1: Isolated full-bridge DC-DC converter

When the circuit is working, the switching tubes *Q1* to *Q4* have driving signals, and only the antiparallel diodes *D1* to *D4* are used to realize the output full-bridge rectification. Each switch is turned on or off with a fixed duty cycle of 50 %. There is a phase difference between the switches on the diagonal of the full bridge, that is the phase-shifting angle φ. The sliding mode control method in this paper is to control the output voltage within the required range by calculating the phase-shifting angle of the switch tube. In order to prevent the upper and lower two switch tubes of the same bridge arm from being turned on at the same time, the control signal of the two switch tubes of the same bridge arm must have a dead time t_d. The state space model of the converter can be obtained as follows (Pandey, 2016)

$$\begin{bmatrix} \dot{i}_L \\ \dot{V}_0 \end{bmatrix} = \begin{bmatrix} 0 & -\frac{1}{L} \\ \frac{1}{C} & -\frac{1}{RC} \end{bmatrix} \begin{bmatrix} i_L \\ V_0 \end{bmatrix} + \begin{bmatrix} \frac{V_{in}}{nL} \\ 0 \end{bmatrix} u \tag{1}$$

It can be seen from Eq(1) that the average value of the leakage inductance current in a period is zero, so it is not included in the further discussion. Where u is the switching signal and is shown in Eq(2).

$$u = \begin{cases} 1 & \text{Q1 and Q4 on or Q2 and Q3 on} \\ 0 & \text{Q1 and Q2 on or Q3 nda Q4 on} \end{cases} \tag{2}$$

3. Design of sliding mode controller

3.1 System modelling

Constructing the state space description equation of converter, as shown in Eq(3).

$$x=\begin{pmatrix}x_1\\x_2\\x_3\end{pmatrix}=\begin{pmatrix}V_{ref}-\beta V_0\\ \frac{d}{dt}(V_{ref}-\beta V_0)\\ \int(V_{ref}-\beta V_0)\end{pmatrix} \tag{3}$$

Where, x_1 is the voltage error, x_2 is the derivative of voltage error and x_3 is the integral of the voltage error, V_{ref} is the reference voltage, and β is the voltage division ratio. Eq(4) is the derivative of Eq(3).

$$\dot{x}=Ax+Bu+D$$
$$\begin{pmatrix}\dot{x}_1\\ \dot{x}_2\\ \dot{x}_3\end{pmatrix}=\begin{pmatrix}0&1&0\\0&\frac{1}{RC}&0\\1&0&0\end{pmatrix}\begin{pmatrix}x_1\\x_2\\x_3\end{pmatrix}+\begin{pmatrix}0\\ \frac{-\beta V_{in}}{nLC}\\0\end{pmatrix}u+\begin{pmatrix}0\\ \frac{\beta V_0}{LC}\\0\end{pmatrix} \tag{4}$$

3.2 Design of sliding surface

According to the state space model, the control functions are shown in Eq(5).

$$u=\begin{cases}1 & S>0\\ 0 & S<0\end{cases} \tag{5}$$

Where S is the sliding surface and its design is shown in Eq(6).

$$S=\alpha_1 x_1+\alpha_2 x_2+\alpha_3 x_3=J^T x \tag{6}$$

Where $J^T=[\alpha_1\ \alpha_2\ \alpha_3]$ is the sliding coefficient. Under any load and input parameter, the sliding mode control is satisfied by selecting the exact value of the sliding coefficient.

3.3 Existence conditions of sliding surface

The control law of Eq(5) satisfies the general requirements of the system's running trajectory to the sliding mode surface. However, in order to determine that the system's running trajectory is maintained on the sliding surface, the system must abide by the existence conditions of the system's progressive stability derived from Lyapunov theorem, that Eq(7)

$$\lim_{s\to 0} S\cdot\frac{dS}{dt}<0 \tag{7}$$

The condition of sliding surface is shown in Eq(8).

$$0<-n\beta L(\frac{\alpha_1}{\alpha_2}-\frac{1}{RC})i_C+nLC\frac{\alpha_3}{\alpha_2}(V_{ref}-\beta V_0)+n\beta V_0<\beta V_{in} \tag{8}$$

3.4 Selection of sliding coefficients

According to the damping ratio ζ and the settling time T_s, the sliding coefficient are obtained. The desired settling time T_s = 5τ (1 % error), where τ denotes natural time constant, Eq(9) shows the sliding coefficient ratio (Sachin and Nayak, 2017).

$$\frac{\alpha_1}{\alpha_2}=\frac{10}{T_S}$$
$$\frac{\alpha_3}{\alpha_2}=\frac{25}{\zeta {T_S}^2} \tag{9}$$

3.5 Derivation of control equations for PWM -based controller

The output switch signal frequency is kept constant by fixing the carrier signal frequency. PWM technology is used in the controller design to make the method have a fixed frequency. From first step, equivalent control signal, u_{eq} is originated using invariance condition and second step, u_{eq} is to translate to duty ratio d of PWM is carried during the derivation process. Eq(10) can be obtained from the $\dot{S} = J^T Ax + J^T B u_{eq} + J^T D = 0$.

$$u_{eq} = -\left[J^T B\right]^{-1} J^T \left[Ax + D\right] \tag{10}$$

Where u_{eq} is a continuous function and $0 < u_{eq} < 1$. The duty ratio *d* is given by Eq(11).

$$0 < d = \frac{v_c}{\hat{v}_{ramp}} < 1$$

$$v_c = u_{eq}{}^* = -n\beta L\left(\frac{\alpha_1}{\alpha_2} - \frac{1}{RC}\right)i_C + nLC\frac{\alpha_3}{\alpha_2}(V_{ref} - \beta V_0) + n\beta V_0 \tag{11}$$

$$\hat{v}_{ramp} = \beta V_{in}$$

Then, v_c is the control signal and $\hat{v}_{ramp}$ is the peak value of the carrier signal.
The equivalent circuit diagram of the converter and the control structure of the sliding mode converter are shown in Figure 2. When there is a large disturbances, the integral term of the control can be controlled in the system. The derivative term of control variable lower the settling time and peak overshoot (Tan et al., 2006).

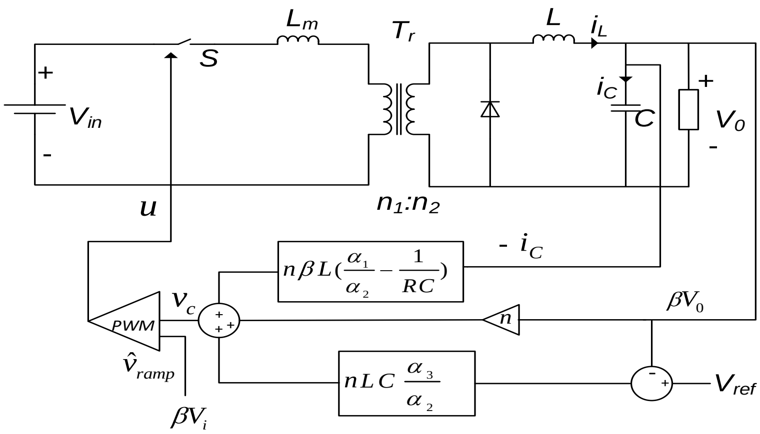

Figure 2: Block diagram of converter equivalent circuit and control structure of sliding mode converter

4. Simulation results

In order to verify the correctness of the theoretical design, this section presents the simulation and experimental results of the isolated DC-DC converter sliding mode controller. MATLAB / Simulink software is used for simulation. The software can automatically find the defects of the control system according to the parameter setting and the performance of the close to the actual equipment. The processing speed of software simulation is faster. Software verification has great advantages in cost and time. Table 1 lists the parameters of the converter circuit.

Table 1: The simulation model of the main parameters

Name	Technical parameters	Name	Technical parameters
input voltage V_{in}	288 V	settling time T_S	80us
capacitor *C*	150 uF	Critical damping ratio ζ	1
inductance *L*	100 uH	reference voltage V_{ref}	2.5 V
load resistance *R*	10 Ω	voltage division ratio *β*	0.208
turns ratio *n*	12	Resonance inductance L_m	2 uF
Frequency f_z	20 kHz	capacitors C_1-C_4	1 nF

When the converter is in the working state of the full-bridge DC converter, the drive signal is only applied to the four switch tubes on the left side. Full-bridge rectification on the secondary side is only achieved by parallel diodes on the switch. The PWM drive waveform of the four switch tubes of the converter are shown in Figure 3. It can be found that there is a dead time between the upper and lower switch tubes of the same bridge arm of the converter. The converter realizes soft switching of the switch tube under sliding mode control.

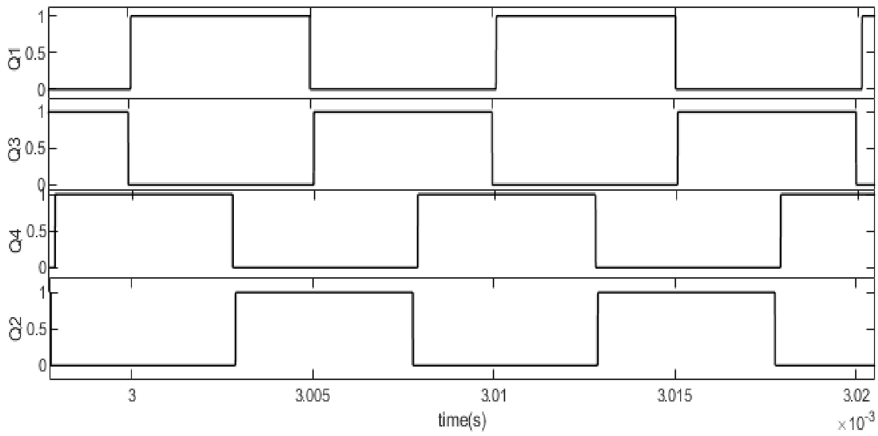

Figure 3: PWM drive signal waveform of the switch

In order to test the robustness of the converter in the disturbed state. When setting 0 - 0.02 s, the load resistance value is 10 Ω, and the resistance value of 0.02 - 0.03 s changes from 10 Ω to 30 Ω. The output voltage waveform obtained by two different control methods is shown in Figure 4.

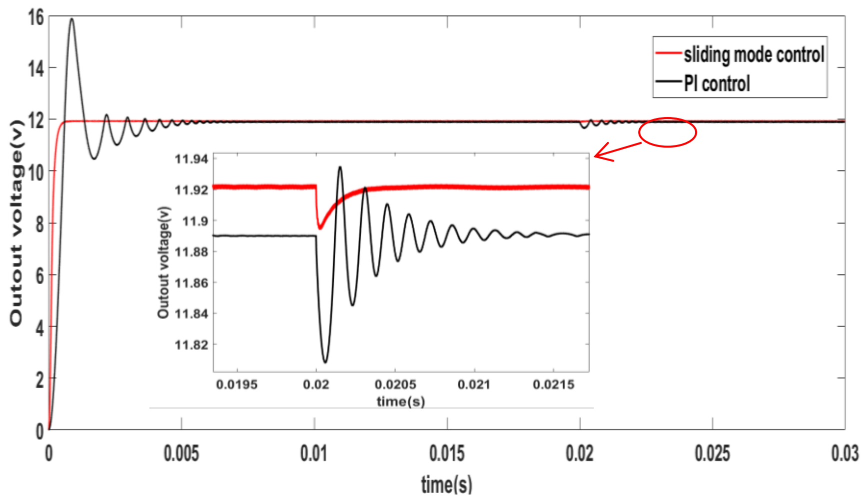

Figure 4: Output voltage when load resistance changed

It can be seen from Figure 4 that the output voltage can quickly track the reference value of 12 V by using sliding mode control. When the load suddenly changes, the output voltage can be restored to a stable value output in a short time. When PI control is adopted, the output voltage response is slow and the overshoot is large, and the output voltage fluctuates greatly when it is interfered by load resistance. When the input voltage changes from 288 V to 350 V in 0.02 s, the output voltage waveform obtained by two different control methods is shown in Figure 5. It can be seen from the comparison that the output voltage of the system is not sensitive to the change the input voltage by using sliding mode control. However, the deviation between the voltage obtained by PI control and the reference value is large, and the response speed of the system is relatively slow.

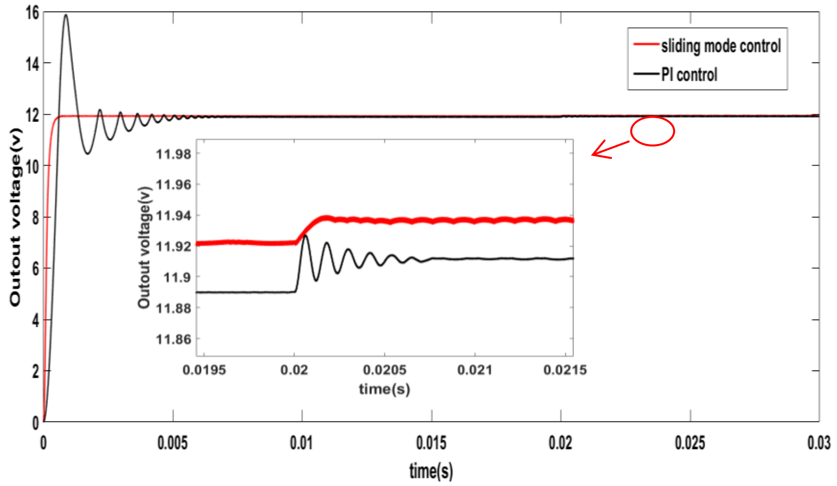

Figure 5: Output voltage when input voltage changed

5. Conclusions

A sliding mode variable structure control strategy is proposed for isolated full bridge DC-DC converter with variable input voltage and load resistance. The output voltage of the converter can track the reference voltage. The selection of sliding surface, existence and stability, and the selection of control parameters are studied. The correctness of the control method is proved by theoretical analysis. Then the MATLAB / Simulink software is introduced, through simulation verification is carried out, compared with the traditional PI control, the correctness of the proposed method and the superiority of the control performance are verified. The simulation results show that the sliding mode control has high precision, faster response speed and lower voltage overshoot, and strong robustness under large input voltage disturbance and load disturbance.

References

Ding S., Zheng W.X., Sun J., Wang J., 2018, Second-order sliding-mode controller design and its implementation for buck converters, in IEEE Transactions on Industrial Informatics, 14(5), 1990-2000

Matwankar C. S., Alam A., 2019, Solar powered closed-loop current controlled DC-DC Buck Converter for Battery Charging Application, 2019 International Conference on Vision Towards Emerging Trends in Communication and Networking (ViTECoN), Vellore, India, 1-5

Na W., Lee H., 2011, Sliding mode control design of current fed full bridge DC to DC converter for fuel cell applications, 2011 IEEE Power and Energy Conference at Illinois, Champaign, America, 1-4

Naik B. B., Mehta A. J., 2017, Sliding mode controller with modified sliding function for DC-DC Buck Converter, ISA transactions,70, DOI: 10.1109/MSMC.2017.2663559

Pandey S. K., 2016, Disturbance observer based sliding mode control for DC-DC power converters, IECON 2016 - 42nd Annual Conference of the IEEE Industrial Electronics Society, Florence, Italy, 3366-3371

Sachin C. S., Nayak S. G., 2017, Design and simulation for sliding mode control in DC-DC boost converter, 2017 2nd International Conference on Communication and Electronics Systems (ICCES), Coimbatore, India, 440-445

Tan S. C., Lai Y. M., Tse C. K., 2006, A unified approach to the design of PWM-based sliding-mode voltage controllers for basic DC-DC converters in continuous conduction mode, in IEEE Transactions on Circuits and Systems, 53(8), 1816-1827, DOI: 10.1109/TCSI.2006.879052.

Yao C., Ruan X.B., Wang X.H, 2015, Automatic mode-shifting control strategy with input voltage feed-forward for full-bridge- boost DC–DC converter suitable for wide input voltage range, IEEE Transactions Power Electronics, 30(3), 1668-1682, DOI: 10.1109/TPEL.2014.2317795

Yu X., Kaynak O., 2017, Sliding Mode Control Made Smarter: A Computational Intelligence Perspective, in IEEE Systems, Man, and Cybernetics Magazine, 3(2), 31-34

Zheng T., 2018, Fault diagnosis of overcharge and overdischarge of lithium ion batteries , Chemical Engineeri ng Transactions,71,1453-1458